Research Article

Argyrin B, a non−competitive inhibitor of the human immunoproteasome exhibiting preference for β1i

AQ1

Duncan J. Allardyce, [1]

Celia M. Bell, [1]

Eriketi Z. Loizidou, [1,✉]

Email e.loizidou@mdx.ac.uk

AQ2

AQ3

[1] Department of Natural Sciences, Faculty of Science and Technology, Middlesex University, London, UK

Correspondence

Eriketi Z. Loizidou, Department of Natural Sciences, Faculty of Science and Technology, Middlesex University, The Burroughs, NW4 4BT, London, UK.

Email: e.loizidou@mdx.ac.uk

Abstract

Inhibitors of the proteasome have found broad therapeutic applications; however, they show severe toxicity due to the abundance of proteasomes in healthy cells. In contrast, inhibitors of the immunoproteasome, which is upregulated during disease states, are less toxic and have increased therapeutic potential including against autoimmune disorders. In this project, we report argyrin B, a natural product cyclic peptide to be a reversible, non−competitive inhibitor of the immunoproteasome. Argyrin B showed selective inhibition of the β5i and β1i sites of the immunoproteasome over the β5c and β1c sites of the constitutive proteasome with nearly 20−fold selective inhibition of β1i over the homologous β1c. Molecular modelling attributes the β1i over β1c selectivity to the small hydrophobic S1 pocket of β1i and β5i over β5c to site−specific amino acid variations that enable additional bonding interactions and stabilization of the binding conformation. These findings facilitate the design of immunoproteasome selective and reversible inhibitors that may have a greater therapeutic potential and lower toxicity.

Graphical Abstract

Reversible inhibitors of the immunoproteasome show great therapeutic potential and lower toxicity. Argyrin B is a non−competitive inhibitor of the immunoproteasome and shows selective inhibition of the β1i site over the homologous β1c site of the constitutive proteasome. Molecular modelling attributes selectivity to site−specific amino acid variations that affect the size and chemical properties of the individual active sites.

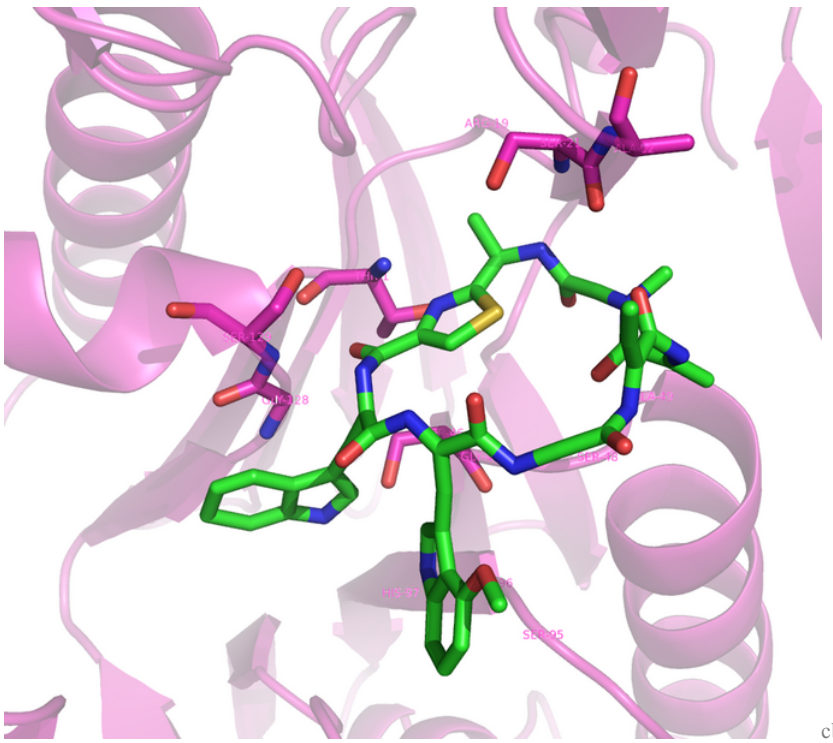

cbdd13539-blkfxd-0001

AQ4

Keywords

argyrin B
docking
immunoproteasome

non−competitive binding
selective inhibitors

1. INTRODUCTION

Protein degradation is involved in the regulation of key pathways such as cell cycle control, DNA repair and apoptosis, where the ubiquitin–proteasome system is the main pathway for the degradation of cytosolic proteins deemed redundant, misfolded or toxic (Ciechanover, 2005; Suh et al., 2013). The 20S core of the proteasome contains the three proteolytic sites through which proteins are cleaved into oligopeptides by the chymotrypsin (β5)−, trypsin (β2)− and caspase (β1)−like activities (Heinemeyer, Ramos, & Dohmen, 2004; Orlowski & Wilk, 2000). Inhibitors of the proteasome act in one or more of the active sites and have shown broad therapeutic applications, particularly for multiple myeloma and mantle cell lymphoma. However, as the proteasome is required for normal cell function, its inhibition becomes associated with severe toxicity (Crawford, Walker, & Irvine, 2011; Genin, Reboud−Ravaux, & Vidal, 2010; Goldberg, 2012; Kisselev, van der Linden, & Overkleeft, 2012; Kuhn et al., 2007; Moore, Eustáquio, & McGlinchey, 2008; Parlati et al., 2009; Pellom & Shanker, 2012; Shah, Biran, & Vesole, 2016; Shivakumar & Jagganath, 2006; Sun et al., 2015; Teicher & Tomaszewski, 2015; Wu et al., 2010; Zhang et al., 2014, 2016). Cells in disease states, where the demand for protein degradation is higher, are capable of producing immunoproteasomes in which the catalytic β1c, β2c and β5c subunits of the constitutive proteasome are replaced by the homologous β1i, β2i and β5i whilst all other subunits remain unchanged (Kniepert & Groettrup, 2014; Yewdell, 2005). As a result of these structural changes, the cleavage specificities of the immunoproteasome and constitutive proteasome differ and immunoproteasome preferentially cleaves after hydrophobic amino acids (Gaczynska, Rock, Spies, & Goldberg, 1994). Besides the constitutive proteasome and immunoproteasome, two additional intermediate subtypes exist, which contain a mixture of constitutive and immunoproteasome subunits, that is either immunosubunit β5i, and constitutive subunits β1ic and β2c, or immunosubunits β1i and β5i, and constitutive subunit β2c. Intermediate proteasomes are abundant in normal tissues (between one−third and one−half of total proteasome content) and are also present in human tumour cells (10%–20%) and dendritic cells (30%–50%) and exhibit trypsin− and chymotrypsin−like activities that are in−between those of the constitutive and the immunoproteasome. As such, intermediate proteasomes produce a unique set of antigenic peptides, and together with the immunoproteasome, they represent valuable targets for cancer immunotherapy (Dahlmann, Ruppert, Kuehn, Merforth, & Kloetzel, 2000; Guillaume et al., 2010, 2012; Vigneron & Van den Eynde, 2014).

Most existing proteasome inhibitors block the active sites of both the constitutive proteasome and immunoproteasome at similar potencies (Bakas et al., 2018; Kuhn & Orlowski, 2012; Parlati et al., 2009). However, significant advancements in crystal structure elucidations have enabled the identification of sufficient structural differences in the binding pockets of the different forms of proteasomes (Groll, Berkers, Ploegh, & Ovaa, 2006; Harshbarger, Miller, Diedrich, & Sacchettini, 2015; Huber et al., 2012; Santos et al., 2017) to allow for selective structure−based drug design and selective inhibition. These structural differences have allowed the design of peptide epoxyketone derivatives (Carmony et al., 2012; Ho, Bargagna−Mohan, Wehenkel, Mohan, & Kim, 2007) and peptidyl boronate ML604440 (Basler et al., 2012) that bind specifically at the β1i site. Furthermore, oxathiazolones have been reported to inhibit β5i with a remarkable 4,700−fold selectivity over the constitutive proteasome (Fan, Angelo, Warren, Nathan, & Lin, 2014). Peptide epoxyketones represent another class of β5i selective inhibitors (de Bruin et al., 2014; Dubiella et al., 2014; Fan et al., 2014; Groll, Korotkov, Huber, de Meijere, & Ludwig, 2015; Koroleva et al., 2015) amongst which PR−957, an analogue of carfilzomib, shows 20− to 40−fold selectivity towards β5i in MOLT−4 cells where both forms of the proteasome are expressed and showed evidence of disease reversal of rheumatoid arthritis mouse models (Muchamuel et al., 2009). PR−924, a selective inhibitor of the immunoproteasome with up to 250−fold selectivity towards β5i over β5c (Huber, Heinemeyer, de Bruin, Overkleeft, & Groll, 2016), selectively inhibited growth and triggered apoptosis in multiple myeloma cells over normal cells, validating the β5i site as a target for multiple myeloma treatment (Singh et al., 2011). These inhibitors are irreversible and covalently modify the active site threonine forming a protein–drug adduct. Landsteiner and Jacobs over 80 years ago (Landsteiner & Jacobs, 1935) discovered a direct association between a chemical's propensity to bind covalently to protein and immune sensitization with the risk of developing idiosyncratic adverse drug reactions (Zhou, Chan, Duan, Huang, & Chen, 2005). From this perspective, reversible inhibitors can offer an advantage as they can potentially inhibit at low nanomolar concentrations without producing protein adducts that trigger drug hypersensitivity. Recently, reversible β5i selective inhibitors have been reported to selectively induce cell death in malignant myeloma cells (Santos et al., 2017) and to promote long−term acceptance of cardiac allografts in mice by regulating immune activity (Sula Karreci et al., 2016).

AQ5

Argyrins are a family of cyclic peptides derived from the myxobacterium Archangium gephyra analogues of which have shown to be potent, reversible inhibitors of the constitutive proteasome with mechanisms distinct to existing therapeutics (Bülow et al., 2010; Ferrari et al., 1996; Loizidou & Zeinalipour−Yazdi, 2014; Selva et al., 1996; Stauch et al., 2010). Argyrin B (Figure 1), initially discovered in screening for antibiotics, has displayed some antibacterial as well as antifungal activities (Nyfeler et al., 2012). In human B cells, argyrin B exhibited immunoglobulin G inhibition and showed reduced activity of T and B lymphocytes in murine studies, highlighting its strong immunosuppressive effects (Sasse et al., 2002). Taking into consideration both the proteasome inhibition and immunosuppressive effects of argyrin B, in this project, we wished to further investigate the potential for selective inhibition of the immunoproteasome. Active site inhibition of the β5c and β1c subunits of the constitutive proteasome and the β5i and β1i subunits of the immunoproteasome were investigated using purified enzyme assays alongside molecular modelling. Kinetic assays revealed that argyrin B selectively inhibits β1i over β1c with 20−fold selectivity and shows low micromolar K_i values for both β1i and β5i. Molecular modelling simulations reveal that the increased hydrophobicity and smaller size of the β1i S1 pocket contribute to the selective binding of argyrin B whilst the site−specific amino acid variation A27S (from β5c to β5i) enables additional hydrogen bonding at the β5i site that may further stabilize binding compared to β5c.

Fig. 1

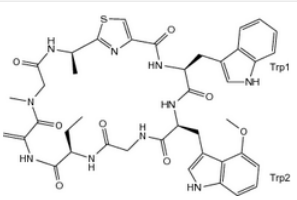

Chemical structure of argyrin B

2. METHODS AND MATERIALS

2.1. Material

20S proteasome (purified human erythrocyte), 20S immunoproteasome (purified human enzyme), NBS 96−well microplates, 7−amino−4−methylcoumarin (AMC) standards, Z−Leu−Leu−Glu−AMC, Suc−Leu−Leu−Val−Tyr−AMC, epoxomycin, sodium dodecyl sulphate and vinyl sulphone (Ada−(Ahx3)−(Leu)3−vinyl sulphone) were purchased from Enzo Life Sciences, Exeter, UK. Ac−Pro−Ala−Leu−AMC was purchased from Bio−Techne, Abingdon, UK, dimethyl sulphoxide (DMSO) from Fisher Scientific, Loughborough, UK, and Argyrin B was a donation from Novartis.

2.2. **Purified enzyme assays**

Substrate and inhibitor reagents were dissolved in DMSO for stock solutions and subsequently diluted in proteasome assay buffer to desired concentrations. Assay reagents were added to 96−well plates to a final volume of 50 µl per well, throughout. Concentrations of the 20S proteasome and 20S immunoproteasome were maintained constant at 0.1 µg/well. AMC standards were prepared from a 1:2 serial dilution of 8 to 0.25 µM and blank. All purified enzyme reactions were performed at 37°C, and the liberation of AMC was measured over time using a BMG Labtech fluorescence plate reader set at 355/460 nm (excitation/emission). Positive controls were performed by the reaction of proteasome or immunoproteasome with active site−specific substrates: Z−LLE−AMC (β1), Ac−PAL−AMC (β1i) and Suc−LLVY−AMC (β5/β5i). Negative controls were performed using epoxomycin a potent inhibitor of β5/β5i and vinyl sulphone a potent inhibitor of β1/β1i. Blanks were performed with substrate only, and additional controls for solvent (DMSO) concentration were used where applicable.

Using 0.1 µg/well of enzyme, a range of at least seven substrate concentrations were used to generate Michaelis–Menten plots for Michaelis–Menten constant (K_m) analysis at each active site. Subsequent K_m values were used as the single substrate concentration in IC_{50} plots that covered a logarithmic range of at least 10 argyrin B concentrations. For kinetic assays to determine inhibition constant (K_i), the following inhibitor and substrate concentrations were used: argyrin B concentrations ranged from estimated IC_{50} value (β1c = 183.7 µM, β1i = 10.4 µM, β5 = 11.4 µM, β5i = 10.3 µM) × 0, 0.33, 1 and 3, whilst substrate concentration covered K_m (β1 = 95.4 µM, β1i = 69.9 µM, β5 = 72.4 µM, β5i = 89.8 µM) × 2.5, 1.25, 0.625, 0.3125 and 0.15625.

Assays were performed with triplicates at every control and concentration variant. For each replicate, the initial rate of reaction was determined from the linear phase of the graph at which less than 10% of substrate had been consumed. GraphPad Prism 6 non−linear curve fitting analysis was used for calculation of K_m, IC_{50} and K_i values. For K_m, a Michaelis–Menten plot was the preferred model, whilst for IC_{50} analysis, a normalized response curve was fit against logarithmic inhibitor concentration allowing for variable slope function. Data are reported with mean, SEM and 95% confidence interval. A standard, unpaired, t test was used to analyse significance between the three IC_{50} value repeats of argyrin B at different active sites at 95% confidence level. Alongside K_m and V_{max} values, Akaike's information criterion (AICc) (Motulsky & Christopoulos, n.d.) and the F test hypothesis testing approach at $p < 0.05$ were used to determine the best−fit simultaneous non−linear regression analysis model between competitive, non−competitive, uncompetitive and mixed inhibition that subsequently calculated K_i. Estimates of the inhibition constant K_i are reported with SEM and 95% confidence intervals.

2.3. **Computational methods**

All 3−dimensional structures were obtained from RCSB Protein Data Bank and prepared using the molecular graphics package PYMOL (v1.7.4.5). An argyrin B structure was isolated from PDB:4FN5 (Nyfeler et al., 2012) and its geometry optimized using the molecular mechanics with UFF force field function of Avogadro (Hanwell et al., 2012). The human constitutive 20S proteasome structural data were available from PDB:4R3O (Harshbarger et al., 2015). β1, β2 and β5 active sites were cut for residues within 28 Å from the catalytic Thr1 position of each active subunit chain from the same β−ring on the same monomer using PyMOL. IP structural data were obtained from PDB:3UNH (Huber et al., 2012) murine IP and subsequently modified in order to create a humanized IP model as follows: human active site sequences for β1i, β2i and β5i (UniProt: P28065, P40306 and P28062, respectively) were aligned to murine immunoproteasome FASTA sequences using EMBL−EBI Clustal Omega and EMBOSS Smith–Waterman alignment algorithm followed by identification of the conserved amino acids. Subsequently, the amino acid mutation utility of SWISSPDB VIEWER (v.4.10) was used to mutate variable, individual amino acids of murine IP to those of the corresponding human IP. Active sites were subsequently cut as described for the constitutive proteasome.

AUTODOCK (v.4.2.6) was used to simulate argyrin B binding (Morris et al., 2009) at the active sites of the immunoproteasome and constitutive proteasome. The grid box was set at 70x, 70y, 70z dimensions, centred based on Thr1 co−ordinates on the active subunit chains as follows: 23.238, −78.082, −11.152 for β1i, 52.961, −24.734, −1.942 for β5i and −44.697, 77.350, −80.590 for β1c, −42.794, 25.372, −104.397 for β5c.

Argyrin B was allowed rotational freedom at the bonds connecting the tryptophan rings to the peptide cycle, as well as the Trp2−OMethoxy bond whilst the constitutive proteasome and immunoproteasome active sites were treated as non−flexible. A genetic algorithm with 50 runs was selected for all docking experiments. Each docking experiment was repeated 10 times, and for each set of 10 replicate best binding energies, the data were tested for normality where those with $p > 0.05$ show normal distribution. For normally distributed sets, equal variance was tested between each active site. A 2−sample t test was used for those of equal variance, whilst a non−parametric Mann–Whitney test was used for results not of equal variance, to test for significance (p−values of <0.05 show statistical difference).

3. **RESULTS**

3.1. **Kinetic assays**

To assess the inhibitory activity of argyrin B against the immunoproteasome, we performed kinetic assays using recombinant proteasome and immunoproteasome and β1c, β1i, β5c and β5i site−specific substrates (Miller, Ao, Kim, & Lee, 2013). The β2c and β2i sites were excluded from testing since as revealed by the crystal structures their active sites are remarkably similar and thus a difference in the binding affinity of inhibitors towards β2c and β2i is not expected (Huber et al., 2012). To determine the IC_{50} values (Figure 2), the substrate concentration was chosen at the K_m value in order to avoid unrepresentative values from different inhibition modes (Cheng & Prusoff, 1973; Michaelis–Menten plots shown in Figure S1). The highest binding affinity that argyrin B achieved was for the β5i site with an IC_{50} of 3.54 µM, followed by β5c and β1i with IC_{50} of 8.30 and 8.76 µM, respectively. The affinity of argyrin B for the β1c site was much lower with IC_{50} of 146.5 µM, showing a 16−fold selectivity towards β1i over β1c (Table 1). Kinetic analysis further supported our data where the K_i for the β1c site was estimated to be larger than 100 µM (Table 1). An accurate value for the K_i for β1c could not be determined due to the high concentration of argyrin B at 3 × IC_{50} (439.5 µM) that was required to carry out the β1c K_i range tests. At this concentration, the amount of DMSO that is required to dissolve argyrin B is high enough to have a significant impact on enzyme–substrate reaction. Kinetic analysis revealed similar inhibition constants for β1i and β5i with estimated K_i 5.21 and 6.61 µM, respectively, followed by β5c with K_i 13.85 µM. Over 20−fold selectivity of β1i over the β1c site is observed.

Fig. 2

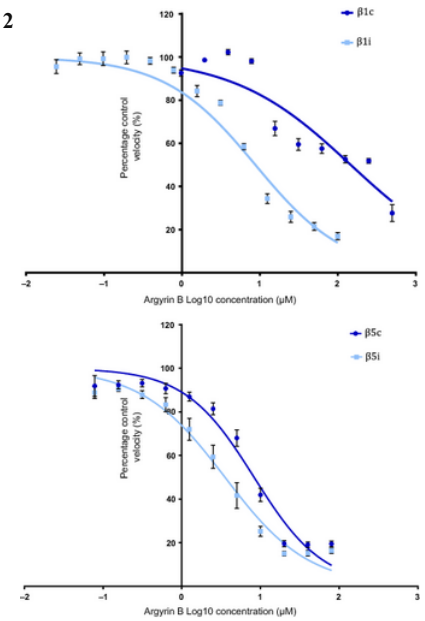

Argyrin B IC_{50} plots at β1c, β1i, β5c, β5i sites. Logarithmic argyrin B concentration against percentage control, initial rate velocity. Tested at [CP] and [IP] = 0.1 μg/well and [S] = K_m (K_m values: β1c = 95.4 μM, β1i = 69.9 μM, β5c = 72.4 μM, β5i = 89.8 μM). Non−linear regression analysis with variable hill slope and $1/y^2$ weighting generated IC_{50} values with respective SEM from 3 independent repeats. (a) β1i IC_{50} = 8.76 μM ±1.08, β1c IC_{50} = 146.5 μM ±1.10. B) β5c = 8.30 μM ±1.07, β5i = 3.54 μM ±1.08. DMSO solvent controls used where applicable

Table 1 Summary of IC_{50} and K_i analysis at β1c, β1i, β5c and β5i

	β1c	**β1i**	**β5c**	**β5i**
IC_{50} (μM)	146.5[a]	8.76	8.30	3.54
SE	1.10	1.08	1.07	1.08
95% CI	122.3–175.5	7.6–10.1	7.8–9.4	3.0–4.1
K_i (μM)	>100	5.21	13.85	6.61
SE	—	0.34	0.96	0.49
95% CI	—	4.54–5.89	11.93–15.76	5.63–7.59

[a]Denotes statistical significance from t test.

K_i values were determined based on a non−competitive model, which proved to be the best fit based on AICc analysis (Kakkar, Pak, & Mayersohn, 2000). The non−competitive model and estimated K_i values were also supported by alternative analysis methods including Cornish–Bowden and Dixon plots as well as a conventional Hanes–Woolf plot (Figures S2–S5).

Despite inhibiting non−competitively, argyrin B can still bind at the active site as reported for other members of the argyrin family (Loizidou & Zeinalipour−Yazdi, 2014; Stauch et al., 2010) as well as the β5c and β5i asparagine−ethylenediamine−based inhibitors (Santos et al., 2017). Non−competitive binding can potentially be beneficial in a cell environment where protein degradation is inhibited leading to progressive accumulation of substrate, as the concentration of substrate would not influence the degree of inhibition.

3.2. **Molecular docking**

Molecular docking was employed to shed light on the possible mechanisms of selective inhibition exhibited by argyrin B towards the immunoproteasome. Based on existing knowledge that argyrin analogues bind near the active site of the proteasome (Stauch et al., 2010), the grid box was centred at the β1i and β5i and β1c and β5c active sites for the molecular docking studies with argyrin B. The active sites were simulated by using the three−dimensional structure for the human constitutive proteasome and a homology model of the human immunoproteasome that was generated using the crystal structure of the mouse immunoproteasome as the template (Figures S6, S7 and Table S1). Compared to the β1c active site, β1i is smaller in size and has a more hydrophobic character. This is exemplified by the key substitutions from constitutive to immunoproteasome in residues of the S1 specificity pocket, T22V, T33F, R47L, T52A (Figure 3). Apart from the conservative R47L substitution, all others involve changing of a polar amino acid to a hydrophobic amino acid and as such provide a hydrophobic character. Additionally, the β1i site is short of one amino acid, at position 115, which is consistent with the reported sequences for β1i (Huber et al., 2012).

Fig. 3

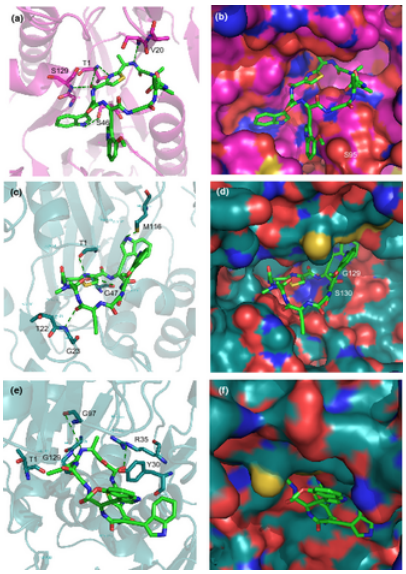

Best-docked conformations of argyrin B (shown as stick representation) at the β1i (a and b) and β1c (c–f) active sites. (a) Best-docked conformation of argyrin B at β1i active site, enzyme is shown as magenta cartoon representation. Hydrogen-bonding interactions between argyrin B and amino acids Thr1, Ser21, Ser46 and Ser129 are shown as green dotted lines. (b) Best-docked conformation of argyrin B at β1i active site, enzyme is shown as surface representation where colours red, blue, yellow and magenta correspond to oxygen, nitrogen, sulphur and carbon elements; (c) best-docked conformation 1 of argyrin B at β1c active site, enzyme is shown as teal cartoon representation. Hydrogen-bonding interactions between argyrin B and amino acids Thr1, Gly47, Thr22 and Met116 are shown as green dotted lines; (d) best-docked conformation 1 of argyrin B at β1c active site, enzyme is shown as surface representation where colours red, blue, yellow and teal correspond to oxygen, nitrogen, sulphur and carbon elements. (e) Best-docked conformation 2 of argyrin B at β1c active site, enzyme is shown as teal cartoon representation. Hydrogen-bonding interactions between argyrin B and amino acids Arg35, Gly97 and Gly128 are shown as green dotted lines; (f) best-docked conformation 2 of argyrin B at β1c active site, enzyme is shown as surface representation where colours red, blue, yellow and teal correspond to oxygen, nitrogen, sulphur and carbon elements

The binding of argyrin B at both β1i and β1c sites was found to be mainly driven by VdW, hydrogen-bonding and desolvation interactions with argyrin B displaying a significant difference in binding preference towards β1i (−11.83 kcal/mol) compared to β1c (−10.12 and −9.74 kcal/mol). One main binding conformation was identified at the β1i site showing great consistency of interactions between argyrin B and amino acids of the β1i active site. Argyrin B is positioned close to Thr1, which participates in two hydrogen-bonding interactions with the thiazole nitrogen of argyrin B as well as an additional hydrogen bond with the adjacent carbonyl oxygen. The latter is further stabilized by a hydrogen bond with Ser129. Additional hydrogen bonding was identified between trp 1 of argyrin B and Ser46 as well as between an amide backbone of the argyrin macrocycle and Val 20. VdW interactions were identified between argyrin B and the amino acids Ala49, Arg19, His97, Met5, Ser48, Val20, Gly128, Gly47, Ala96, Leu115 and Tyr30. Additionally, Ser95 is likely to be involved in dipole–dipole interactions with trp 2 of argyrin B.

In contrast, molecular modelling suggested a dual binding mode for argyrin B at the active site of β1c, where interactions with residues Arg35, Gly47, Met116 and Met95 appear in both conformations. The two binding conformations appear at a 2:3 ratio. At the more abundant binding conformation 1 (Figure 3c,d), argyrin B is positioned close to Thr1 forming a similar hydrogen bond with the thiazole ring which is further stabilized through a second hydrogen bond with Gly47. Additional hydrogen-bonding interactions were identified between the amino acids Thr22 and backbone carbonyl of argyrin B as well as Met116 and trp2. Trp1 is surrounded by residues Arg35, Gly97, Gly129, Ser130 and Ser46 forming VdW interactions. Additional VdW interactions were between the amino acids Thr20, Thr21, Gly23, Ala49, Met95, and Val20 and the cyclic backbone of argyrin B.

In the less frequently occurring but more energetically favoured (−10.12 kcal/mol compared to −9.74 kcal/mol) conformation 2, argyrin B is positioned further away from Thr1 enabling aromatic interactions between Tyr30 and the tryptophan rings of argyrin B (Figure 3e–f). Hydrogen-bonding interactions are observed with amino acids Arg35, Gly97, and Gly128 and VdW interactions with amino acids Gly129, Pro115, Met116, Gly47, Met95, Met5, Tyr30, Leu33, Ser133, at β1c.

Overall, there are five hydrogen-bonding interactions in β1i compared to four hydrogen-bonding interactions in β1c conformation 1, offering the extra stabilization. It is likely that the more compact size of the β1i site compared to the β1c allows for a better fit for argyrin B and the facilitation of interactions with amino acids of the active site. On the other hand, the more spacious β1c site allows argyrin B to adopt several binding conformations and this is exemplified by the two main binding modes identified by molecular modelling.

Similarly to the β1 sites, the binding of argyrin B at both β5i and β5c sites was found to be mainly driven by VdW, hydrogen-bonding and desolvation interactions. One main binding conformation was identified at the β5i site showing great consistency of interactions between argyrin B and amino acids of the β5i active site (Figure 4a,b). Four main hydrogen-bonding interactions were identified with residues Thr1, Ser21 and Ser46. VdW interactions were identified with amino acids Val31, Ala49, Met45 and Lys33, which surround trp1 of argyrin B as well as amino acids Gly47, Gly129 and Tyr169.

Fig. 4

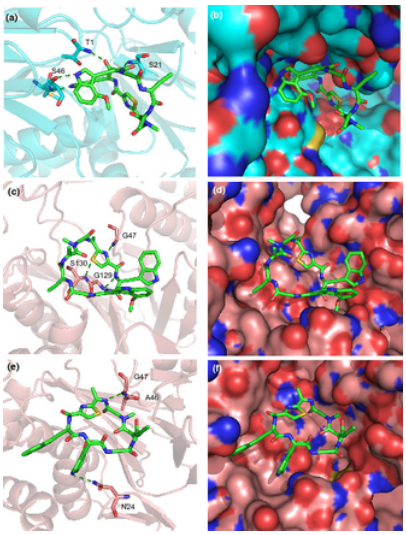

Best-docked conformations of argyrin B (shown as stick representation) at the β5i (a and b) and β5c (c–f) active sites. (a) Best-docked conformation of argyrin B at β5i active site, enzyme is shown as light blue cartoon representation. Hydrogen-bonding interactions between argyrin B and amino acids Thr1, Ser21 and Ser46 are shown as green dotted lines. (b) Best-docked conformation of argyrin B at β5i active site, enzyme is shown as surface representation where colours red, blue, yellow and light blue correspond to oxygen, nitrogen, sulphur and carbon elements; (c) best-docked conformation 1 of argyrin B at β5c active site, enzyme is shown as light pink cartoon representation. Hydrogen-bonding interactions between argyrin B and amino acids Gly47, Gly129 and Ser130 are shown as green dotted lines; (d) best-docked conformation 1 of argyrin B at β5c active site, enzyme is shown as surface representation where colours red, blue, yellow and light pink correspond to oxygen, nitrogen, sulphur and carbon elements. (e) Best-docked conformation 2 of argyrin B at β5c active site, enzyme is shown as light pink cartoon representation. Hydrogen-bonding interactions between argyrin B and amino acids Asn24 and Gly47 are shown as green dotted lines; (f) best-docked conformation 2 of argyrin B at β5c active site, enzyme is shown as surface representation where colours red, blue, yellow and light pink correspond to oxygen, nitrogen, sulphur and carbon elements

A dual binding mode was identified at the β5c site of the constitutive proteasome. In β5c, the frequency of appearance of the two main conformations follows a similar pattern to β1c, that is a 2:3 ratio for β5c conformation 1 (binding energy −10.52 kcal/mol) vs β5c conformation 2 (binding energy −10.72 kcal/mol) where both conformations show similar binding energies. In both binding conformations, argyrin B binds in a similar area but the tryptophan rings are positioned on opposite sites (Figure 4c–f). In conformation 1 (Figure 4c), argyrin B forms three hydrogen-bonding interactions with Gly47, Gly129 and Ser130. The remaining interactions are VdW with amino acids Thr1, Ser96, Ser116, Asp115, Tyr113, Glu117, Ser23, Asn24, Tyr134, Ala32, Asp167 and Tyr169. In this conformation, the tryptophan rings of argyrin B are interacting primarily with polar amino acids including Ser96, Ser116, Asp115, Glu117 and Tyr113 in which the hydroxyl group is facing towards the tryptophan rings.

In conformation 2 (Figure 4e), argyrin B forms two hydrogen-bonding interactions with Gly47 and Asn24. The remaining interactions are VdW with amino acids Val133, Phe137, Gln33, Ile30, Ala32, Tyr169, Ser130, Gly129, Val128, Thr1, Ala46, Gly98, Glu117 and Tyr113. In this second conformation, trp1 of argyrin B is surrounded by residues Tyr169, Ala32, Gln33, Ile30 and Phe137 forming primarily hydrophobic interactions.

The energetics of binding are similar for β5i and β5c. In β5i, all bonding is based around the Trp moieties whilst no residues strongly interacted at the opposing end of the inhibitor. The tryptophan rings of argyrin B wrapped around Ser46, each forming hydrogen bonds. Argyrin B interacted with residues only from the β5i subunit in the immunoproteasome, whereas conformations within the constitutive proteasome also displayed interactions with nearby subunit chains, that is Ser23 and Asn24 from the neighbouring β4 and Ala32 from β3.

Comparing the β5 sites of both the human constitutive and immunoproteasomes (Figure S8), they appear to be remarkably conserved amongst key residues that confer chymotrypsin-like activity Ala20, Met45, Ala49 and Cys52 (Huber et al., 2012); however, the substitutions at the key residues, A46S and T128V (from β5c to β5i) surrounding Thr1, as well as the G48C (from β5c to β5i) substitution at the S3 pocket, give the β5i site a more polar character and also have a role in defining the shape of the active site (Huber et al., 2012). Keeping this in mind, the A27S substitution enables the formation of the hydrogen bond between argyrin B and S27 at the β5i site, which is not possible with A27 at β5c. Overall however, the predicted binding energies of argyrin B are not statistically different over the two β5 sites (Table 2).

Table 2 Comparison of estimated binding energies from molecular modelling and inhibition constants from kinetic assays

	β1		**β5**	
	CP	**IP**	**CP**	**IP**
Lowest binding energy (kcal/mol)	−9.74 (conf. 1) −10.12 (conf. 2)	−11.83	−10.52 (conf.1) −10.72 (conf.2)	−10.97
Average binding energy (kcal/mol)	−9.81	−11.66	−10.58	−10.73
SE	0.062	0.045	0.027	0.056
Calculated K_i from assays (μM)	>100	5.21	13.85	6.61

4. DISCUSSION

Argyrins are known inhibitors of the constitutive proteasome that bind reversibly at the active site (Loizidou & Zeinalipour−Yazdi, 2014). In this study, we showed that argyrin B inhibits the constitutive proteasome and immunoproteasome non−competitively and shows greater selectivity towards the β1i site of the immunoproteasome with IC_{50} and K_i values at low μM range. Within the immunoproteasome, argyrin B did not show subunit selectivity as both β5i and β1i are inhibited with similar potency. This is potentially advantageous as studies have shown that the cytotoxicity of proteasome inhibitors does not correlate with β5 inhibition and that the simultaneous inhibition with either β1 or β2 is needed to reduce protein degradation (Britton et al., 2009; Kisselev, Callard, & Goldberg, 2006; Weyburne et al., 2017). This is further supported by the study of Britton et al. who showed that maximal cytotoxicity in cells is achieved when proteasome inhibitors target more than one sites (Britton et al., 2009). A possible explanation for this is allosteric interactions between active sites in which inactivation of one site by an inhibitor would lead to the other two sites compensating for loss of activity (Kisselev, Akopian, Castillo, & Goldberg, 1999). To this end, Weyburne et al. (2017) showed that co−inhibition of β2 enhances the inhibitory activity of FDA−approved β5 proteasome inhibitors to triple−negative breast cancer cells, by blocking recovery of proteasome activity. These studies support the hypothesis that subunit specific proteasome inhibitors may not lead to clinically useful drugs and that in contrast efforts should be focused on immunoproteasome over proteasome selectivity.

The ability of argyrin B to inhibit all sites of the proteasome has also been documented by Bülow et al. (2010) who also reported an IC_{50} value for argyrin B at 4.6 nM from MTT cytotoxicity assays in SW−480 colon cancer cells. This assay measures overall metabolic activity to reflect cell viability and therefore also reflects the overall effect of inhibition of all proteasome sites. In other words, argyrin B inhibits more than one sites of the proteasome leading to a synergistic effect of each active site inhibition and an overall lower IC_{50} value (4.6 nM). In this project, the possibility of synergistic inhibition could not be evaluated, as the inhibition of each active site was determined independently which also explains the higher IC_{50} values that are observed in this study (Table 1). A strong correlation has been observed between theoretical and experimental studies. Molecular modelling predicts that argyrin B will bind the strongest to β1i, followed by β5i and β5c and last to β1c; this trend is also confirmed from the inhibition kinetics experiments (Table 2). Argyrin B interacts with the β1i and β5i sites of the immunoproteasome with higher affinity than the corresponding sites of the constitutive proteasome. In the case of the immunoproteasome, binding is facilitated by additional hydrogen bonding compared to the constitutive proteasome and this was made possible due to either a better fit within the active site (the case for β1i) or an amino acid variation from constitutive to immunoproteasome, A27S for the case of β5i.

Taken together, these results further highlight the feasibility of designing immunoproteasome selective inhibitors facilitated by molecular modelling. At the same time, the identification of a non−competitive reversible inhibitor of the immunoproteasome with selectivity towards β1i shows great promise for the development of therapeutics associated with reduced toxicity.

5. **ACKNOWLEDGMENTS**

Donation of argyrin B by Novartis is gratefully acknowledged.

6. **CONFLICT OF INTEREST**

The authors declare no conflict of interest.

7. **DATA AVAILABILITY**

The data that support the findings of this study are available from the corresponding author upon reasonable request.

AQ6

Supplementary Material

REFERENCES

Bakas, N. A., Schultz, C. R., Yco, L. P., Roberts, C. C., Chang, C. A., Bachmann, A. S., & Pirrung, M. C. (2018). Immunoproteasome inhibition and bioactivity of thiasyrbactins. Bioorganic & Medicinal Chemistry, 26(2), 401–412. https://doi.org/10.1016/j.bmc.2017.11.048

AQ7

Basler, M., Lauer, C., Moebius, J., Weber, R., Przybylski, M., Kisselev, A. F., … Groettrup, M. (2012). Why the structure but not the activity of the immunoproteasome subunit low molecular mass polypeptide 2 rescues antigen presentation. The Journal of Immunology, 189(4), 1868–1877. https://doi.org/10.4049/jimmunol.1103592

Britton, M., Lucas, M. M., Downey, S. L., Screen, M., Pletnev, A. A., Verdoes, M., … Kisselev, A. F. (2009). Selective inhibitor of proteasome's caspase−like sites sensitizes cells to specific inhibition of chymotrypsin−like sites. Chemistry & Biology, 16(12), 1278–1289. https://doi.org/10.1016/j.chembiol.2009.11.015

Bülow, L., Nickeleit, I., Girbig, A.−K., Brodmann, T., Rentsch, A., Eggert, U., … Kalesse, M. (2010). Synthesis and biological characterization of argyrin F. ChemMedChem, 5(6), 832–836. https://doi.org/10.1002/cmdc.201000080

Carmony, K. C., Lee, D.−M., Wu, Y., Lee, N.−R., Wehenkel, M., Lee, J., … Kim, K.−B. (2012). A bright approach to the immunoproteasome: Development of LMP2/β1i−specific imaging probes. Bioorganic & Medicinal Chemistry, 20(2), 607–613. https://doi.org/10.1016/j.bmc.2011.06.039

Cheng, Y., & Prusoff, W. H. (1973). Relationship between the inhibition constant (K1) and the concentration of inhibitor which causes 50 per cent inhibition (I50) of an enzymatic reaction. Biochemical Pharmacology, 22(23), 3099–3108.

Ciechanover, A. (2005). Intracellular protein degradation: from a vague idea thru the lysosome and the ubiquitin–proteasome system and onto human diseases and drug targetingNobel Lecture 2004, © The Nobel Foundation 2004. Cell Death & Differentiation, 12(9), 1178–1190. https://doi.org/10.1038/sj.cdd.4401692

Crawford, L. J., Walker, B., & Irvine, A. E. (2011). Proteasome inhibitors in cancer therapy. Journal of Cell Communication and Signaling, 5(2), 101–110. https://doi.org/10.1007/s12079-011-0121-7

Dahlmann, B., Ruppert, T., Kuehn, L., Merforth, S., & Kloetzel, P.−M. (2000). Different proteasome subtypes in a single tissue exhibit different enzymatic properties. Journal of Molecular Biology, 303, 643–653. https://doi.org/10.1006/jmbi.2000.4185

de Bruin, G., Huber, E. M., Xin, B.−T., van Rooden, E. J., Al−Ayed, K., Kim, K.−B., … Overkleeft, H. S. (2014). Structure−based design of β1i or β5i specific inhibitors of human immunoproteasomes. Journal of Medicinal Chemistry, 57(14), 6197–6209. https://doi.org/10.1021/jm500716s

Dubiella, C., Cui, H., Gersch, M., Brouwer, A. J., Sieber, S. A., Krüger, A., … Groll, M. (2014). Selective inhibition of the immunoproteasome by ligand−induced crosslinking of the active site. Angewandte Chemie (International Ed. in English), 53(44), 11969–11973. https://doi.org/10.1002/anie.201406964

Fan, H., Angelo, N. G., Warren, J. D., Nathan, C. F., & Lin, G. (2014). Oxathiazolones selectively inhibit the human immunoproteasome over the constitutive proteasome. ACS Medicinal Chemistry Letters, 5(4), 405–410. https://doi.org/10.1021/ml400531d

Ferrari, P., Vékey, K., Galimberti, M., Gallo, G. G., Selva, E., & Zerilli, L. F. (1996). Antibiotics A21459 A and B, new inhibitors of bacterial protein synthesis. II. Structure elucidation. The Journal of Antibiotics, 49(2), 150–154. https://doi.org/10.7164/antibiotics.49.150

Gaczynska, M., Rock, K. L., Spies, T., & Goldberg, A. L. (1994). Peptidase activities of proteasomes are differentially regulated by the major histocompatibility complex−encoded genes for LMP2 and LMP7. Proceedings of the National Academy of Sciences of the United States of America, 91(20), 9213–9217. https://doi.org/10.1073/pnas.91.20.9213

Genin, E., Reboud−Ravaux, M., & Vidal, J. (2010). Proteasome inhibitors: Recent advances and new perspectives in medicinal chemistry. Current Topics in Medicinal Chemistry, 10(3), 232–256. https://doi.org/10.2174/156802610790725515

Goldberg, A. L. (2012). Development of proteasome inhibitors as research tools and cancer drugs. The Journal of Cell Biology, 199(4), 583–588. https://doi.org/10.1083/jcb.201210077

Groll, M., Berkers, C. R., Ploegh, H. L., & Ovaa, H. (2006). Crystal structure of the boronic acid−based proteasome inhibitor bortezomib in complex with the yeast 20S proteasome. Structure, 14(3), 451–456. https://doi.org/10.1016/j.str.2005.11.019

Groll, M., Korotkov, V. S., Huber, E. M., de Meijere, A., & Ludwig, A. (2015). A minimal β−lactone fragment for selective β5c or β5i proteasome inhibitors. Angewandte Chemie (International Ed. in English), 54(27), 7810–7814. https://doi.org/10.1002/anie.201502931

Guillaume, B., Chapiro, J., Stroobant, V., Colau, D., Van Holle, B., Parvizi, G., … Van den Eynde, B. J. (2010). Two abundant proteasome subtypes that uniquely process some antigens presented by HLA class I molecules. Proceedings of the National Academy of Sciences, 107(43), 18599–18604. https://doi.org/10.1073/pnas.1009778107

Guillaume, B., Stroobant, V., Bousquet−Dubouch, M.−P., Colau, D., Chapiro, J., Parmentier, N., … Van den Eynde, B. J. (2012). Analysis of the processing of seven human tumor antigens by intermediate proteasomes. The Journal of Immunology, 189(7), 3538–3547. https://doi.org/10.4049/jimmunol.1103213

Hanwell, M. D., Curtis, D. E., Lonie, D. C., Vandermeersch, T., Zurek, E., & Hutchison, G. R. (2012). Avogadro: An advanced semantic chemical editor, visualization, and analysis platform. Journal of Cheminformatics, 4(1), 17. https://doi.org/10.1186/1758-2946-4-17

Harshbarger, W., Miller, C., Diedrich, C., & Sacchettini, J. (2015). Crystal structure of the human 20S proteasome in complex with carfilzomib. Structure, 23(2), 418–424. https://doi.org/10.1016/j.str.2014.11.017

Heinemeyer, W., Ramos, P. C., & Dohmen, R. J. (2004). Ubiquitin−proteasome system. Cellular and Molecular Life Sciences, 61(13), 1562–1578. https://doi.org/10.1007/s00018-004-4130-z

Ho, Y. K., Bargagna−Mohan, P., Wehenkel, M., Mohan, R., & Kim, K.−B. (2007). LMP2−specific inhibitors: Chemical genetic tools for proteasome biology. Chemistry & Biology, 14(4), 419–430. https://doi.org/10.1016/j.chembiol.2007.03.008

Huber, E. M., Basler, M., Schwab, R., Heinemeyer, W., Kirk, C. J., Groettrup, M., & Groll, M. (2012). Immuno− and constitutive proteasome crystal structures reveal differences in substrate and inhibitor specificity. Cell, 148(4), 727–738. https://doi.org/10.1016/j.cell.2011.12.030

Huber, E. M., Heinemeyer, W., de Bruin, G., Overkleeft, H. S., & Groll, M. (2016). A humanized yeast proteasome identifies unique binding modes of inhibitors for the immunosubunit β5i. The EMBO Journal, 35(23), 2602–2613. https://doi.org/10.15252/embj.201695222

Kakkar, T., Pak, Y., & Mayersohn, M. (2000). Evaluation of a minimal experimental design for determination of enzyme kinetic parameters and inhibition mechanism. The Journal of Pharmacology and Experimental Therapeutics, 293(3), 861–869.

Kisselev, A. F., Akopian, T. N., Castillo, V., & Goldberg, A. L. (1999). Proteasome active sites allosterically regulate each other, suggesting a cyclical bite−chew mechanism for protein breakdown. Molecular Cell, 4(3), 395–402. https://doi.org/10.1016/S1097-2765(00)80341-X

Kisselev, A., Callard, A., & Goldberg, A. L. (2006). Importance of the different proteolytic sites of the proteasome and the efficacy of inhibitors varies with the protein substrate. The Journal of Biological Chemistry, 281(13), 8582–8590. https://doi.org/10.1074/jbc.M509043200

Kisselev, A., van der Linden, W. A., & Overkleeft, H. S. (2012). Proteasome inhibitors: An expanding army attacking a unique target. Chemistry & Biology, 19(1), 99–115. https://doi.org/10.1016/j.chembiol.2012.01.003

Kniepert, A., & Groettrup, M. (2014). The unique functions of tissue−specific proteasomes. Trends in Biochemical Sciences, 39(1), 17–24. https://doi.org/10.1016/j.tibs.2013.10.004

Koroleva, O. N., Pham, T. H., Bouvier, D., Dufau, L., Qin, L., Reboud−Ravaux, M., … Bouvier−Durand, M. (2015). Bisbenzimidazole derivatives as potent inhibitors of the trypsin−like sites of the immunoproteasome core particle. Biochimie, 108, 94–100. https://doi.org/10.1016/j.biochi.2014.11.002

Kuhn, D. J., Chen, Q., Voorhees, P. M., Strader, J. S., Shenk, K. D., Sun, C. M., … Orlowski, R. Z. (2007). Potent activity of carfilzomib, a novel, irreversible inhibitor of the ubiquitin‐proteasome pathway, against preclinical models of multiple myeloma. Blood, 110(9), 3281–3290. https://doi.org/10.1182/blood-2007-01-065888

Kuhn, D. J., & Orlowski, R. Z. (2012). The immunoproteasome as a target in hematologic malignancies. Seminars in Hematology, 49(3), 258–262. https://doi.org/10.1053/j.seminhematol.2012.04.003

Landsteiner, K., & Jacobs, J. (1935). Studies on the sensitization of animals with simple chemical compounds. Journal of Experimental Medicine, 61, 643–656. https://doi.org/10.1084/jem.61.5.643

Loizidou, E. Z., & Zeinalipour‐Yazdi, C. D. (2014). Computational inhibition studies of the human proteasome by argyrin‐based analogues with subunit specificity. Chemical Biology & Drug Design, 84(1), 99–107. https://doi.org/10.1111/cbdd.12298

Miller, Z., Ao, L., Kim, K. B., & Lee, W. (2013). Inhibitors of the immunoproteasome: Current status and future directions. Current Pharmaceutical Design, 19(22), 4140–4151. https://doi.org/10.2174/1381612811319220018

Moore, B. S., Eustáquio, A. S., & McGlinchey, R. P. (2008). Advances in and applications of proteasome inhibitors. Current Opinion in Chemical Biology, 12(4), 434–440. https://doi.org/10.1016/j.cbpa.2008.06.033

Morris, G. M., Huey, R., Lindstrom, W., Sanner, M. F., Belew, R. K., Goodsell, D. S., & Olson, A. J. (2009). AutoDock4 and AutoDockTools4: Automated docking with selective receptor flexibility. Journal of Computational Chemistry, 30(16), 2785–2791. https://doi.org/10.1002/jcc.21256

Motulsky, H., & Christopoulos, A. (n.d.). Fitting models to biological data using linear and nonlinear regression—A practical guide to curve fitting (vol. 4.0).

Muchamuel, T., Basler, M., Aujay, M. A., Suzuki, E., Kalim, K. W., Lauer, C., … Groettrup, M. (2009). A selective inhibitor of the immunoproteasome subunit LMP7 blocks cytokine production and attenuates progression of experimental arthritis. Nature Medicine, 15(7), 781–787. https://doi.org/10.1038/nm.1978

Nyfeler, B., Hoepfner, D., Palestrant, D., Kirby, C. A., Whitehead, L., Yu, R., … Dean, C. R. (2012). Identification of elongation factor G as the conserved cellular target of Argyrin B. PLoS ONE, 7(9), e42657. https://doi.org/10.1371/journal.pone.0042657

Orlowski, M., & Wilk, S. (2000). Catalytic activities of the 20 S proteasome, a multicatalytic proteinase complex. Archives of Biochemistry and Biophysics, 383(1), 1–16. https://doi.org/10.1006/abbi.2000.2036

Parlati, F., Lee, S. J., Aujay, M., Suzuki, E., Levitsky, K., Lorens, J. B., … Bennett, M. K. (2009). Carfilzomib can induce tumor cell death through selective inhibition of the chymotrypsin‐like activity of the proteasome. Blood, 114(16), 3439–3447. https://doi.org/10.1182/blood-2009-05-223677

Pellom, S. T., & Shanker, A. (2012). Development of proteasome inhibitors as therapeutic drugs. Journal of Clinical & Cellular Immunology, Suppl 5, 5.

Santos, R. L. A., Bai, L., Singh, P. K., Murakami, N., Fan, H., Zhan, W., … Lin, G. (2017). Structure of human immunoproteasome with a reversible and noncompetitive inhibitor that selectively inhibits activated lymphocytes. Nature Communications, 8, 1692. https://doi.org/10.1038/s41467-017-01760-5

Sasse, F., Steinmetz, H., Schupp, T., Petersen, F., Memmert, K., Hofmann, H., … Reichenbach, H. (2002). Argyrins, immunosuppressive cyclic peptides from myxobacteria. I. Production, isolation, physico‐chemical and biological properties. The Journal of Antibiotics, 55(6), 543–551. https://doi.org/10.7164/antibiotics.55.543

Selva, E., Gastaldo, L., Saddler, G. S., Toppo, G., Ferrari, P., Carniti, G., & Goldstein, B. P. (1996). Antibiotics A21459 A and B, new inhibitors of bacterial protein synthesis. I. Taxonomy, isolation and characterization. The Journal of Antibiotics, 49(2), 145–149. https://doi.org/10.7164/antibiotics.49.145

Shah, N., Biran, N., & Vesole, D. H. (2016). Ixazomib: An oral proteasome inhibitor for the treatment of multiple myeloma. Expert Opinion on Orphan Drugs, 4(1), 105–113. https://doi.org/10.1517/21678707.2016.1122516

Shivakumar, L., & Jagganath, S. (2006). Novel proteasome inhibitors in multiple myeloma. Clinical Lymphoma and Myeloma, 6(5), 370–372. https://doi.org/10.1016/S1557-9190(11)70415-2

Singh, A. V., Bandi, M., Aujay, M. A., Kirk, C. J., Hark, D. E., Raje, N., … Anderson, K. C. (2011). PR‐924, a selective inhibitor of the immunoproteasome subunit LMP‐7, blocks multiple myeloma cell growth both in vitro and in vivo. British Journal of Haematology, 152(2), 155–163. https://doi.org/10.1111/j.1365-2141.2010.08491.x

Stauch, B., Simon, B., Basile, T., Schneider, G., Malek, N. P., Kalesse, M., & Carlomagno, T. (2010). Elucidation of the structure and intermolecular interactions of a reversible cyclic‐peptide inhibitor of the proteasome by NMR spectroscopy and molecular modeling. Angewandte Chemie International Edition, 49(23), 3934–3938. https://doi.org/10.1002/anie.201000140

Suh, K. S., Tanaka, T., Sarojini, S., Nightingale, G., Gharbaran, R., Pecora, A., & Goy, A. (2013). The role of the ubiquitin proteasome system in lymphoma. Critical Reviews in Oncology/Hematology, 87(3), 306–322. https://doi.org/10.1016/j.critrevonc.2013.02.005

Sula Karreci, E., Fan, H., Uehara, M., Mihali, A. B., Singh, P. K., Kurdi, A. T., … Azzi, J. (2016). Brief treatment with a highly selective immunoproteasome inhibitor promotes long‐term cardiac allograft acceptance in mice. Proceedings of the National Academy of Sciences of the United States of America, 113(52), E8425–E8432. https://doi.org/10.1073/pnas.1618548114

Sun, Q., Xu, B., Niu, Y., Xu, F., Liang, L., Wang, C., … Xu, P. (2015). Synthesis, bioactivity, docking and molecular dynamics studies of furan‐based peptides as 20S proteasome inhibitors. ChemMedChem, 10(3), 498–510. https://doi.org/10.1002/cmdc.201402484

Teicher, B. A., & Tomaszewski, J. E. (2015). Proteasome inhibitors. Biochemical Pharmacology, 96(1), 1–9. https://doi.org/10.1016/j.bcp.2015.04.008

Vigneron, N., & Van den Eynde, B. (2014). Proteasome subtypes and regulators in the processing of antigenic peptides presented by class I molecules of the major histocompatibility complex. Biomolecules, 4(4), 994–1025. https://doi.org/10.3390/biom4040994

Weyburne, E. S., Wilkins, O. M., Sha, Z., Williams, D. A., Pletnev, A. A., de Bruin, G., … Kisselev, A. F. (2017). Inhibition of the proteasome β2 site sensitizes triple‐negative breast cancer cells to β5 inhibitors and suppresses Nrf1 activation. Cell Chemical Biology, 24(2), 218–230. https://doi.org/10.1016/j.chembiol.2016.12.016

Wu, W. K. K., Cho, C. H., Lee, C. W., Wu, K., Fan, D., Yu, J., & Yiu Sung, J. J. (2010). Proteasome inhibition: A new therapeutic strategy to cancer treatment. Cancer Letters, 293(1), 15–22. https://doi.org/10.1016/j.canlet.2009.12.002

Yewdell, J. W. (2005). Immunoproteasomes: Regulating the regulator. Proceedings of the National Academy of Sciences of the United States of America, 102(26), 9089–9090. https://doi.org/10.1073/pnas.0504018102

Zhang, J., Gao, L., Xi, J., Sheng, L., Zhao, Y., Xu, L., … Li, J. (2016). Design, synthesis and biological evaluation of novel non‐covalent piperidine‐containing peptidyl proteasome inhibitors. Bioorganic & Medicinal Chemistry, 24(23), 6206–6214. https://doi.org/10.1016/j.bmc.2016.10.002

Zhang, J., Han, M., Ma, X., Xu, L., Cao, J., Zhou, Y., … Hu, Y. (2014). Design, synthesis and biological evaluation of peptidyl epoxyketone proteasome inhibitors composed of β‐amino acids. Chemical Biology & Drug Design, 84(5), 497–504. https://doi.org/10.1111/cbdd.12342

Zhou, S., Chan, E., Duan, W., Huang, M., & Chen, Y. (2005). Drug bioactivation covalent binding to target proteins and toxicity relevance: Drug metabolism reviews. Drug Metabolism Reviews, 37(1), 41–213. https://doi.org/10.1081/DMR-200028812